

Restriction/Classification
Cancelled

NACA

RESEARCH MEMORANDUM

COMPONENT PERFORMANCE INVESTIGATION OF

J71 TYPE II TURBINES

V - INTERNAL FLOW CONDITIONS OF J71 TYPE IIA TURBINE

By Harold J. Schum, Elmer H. Davison, and Donald A. Petrash

Lewis Flight Propulsion Laboratory
Cleveland, Ohio

Restriction/Classification Cancelled

Restriction/Classification Cancelled

CLASSIFIED

Restriction/
Classification Cancelled

... material contains information affecting the
of the espionage laws, Title 18, U.S.C., Secs. 793
manner to unauthorized person is prohibited by law.

thin the meaning
of which in any

NATIONAL ADVISORY COMMITTEE
FOR AERONAUTICS

WASHINGTON

SEP 22 1955

CONFIDENTIAL CANCELLED

FILE COPY
To be returned to
the files of the National
Advisory Committee
for Aeronautics
Washington, D. C.

CLASSIFICATION CANCELLED
Authority NACA PUBLICATIONS
ANNOUNCEMENTS NO.
Date By

NATIONAL ADVISORY COMMITTEE FOR AERONAUTICS

RESEARCH MEMORANDUM

COMPONENT PERFORMANCE INVESTIGATION OF J71 TYPE II TURBINES

V - INTERNAL FLOW CONDITIONS OF J71 TYPE IIA TURBINE

By Harold J. Schum, Elmer H. Davison, and Donald A. Petrash

SUMMARY

An experimental investigation of the internal flow conditions of the J71 Type IIA turbine was conducted at the equivalent design speed and work output. Results indicate that the first stage produced 42 percent of the total work, the second stage 33 percent, and the third stage 25 percent. These experimental values closely correlated the design values of 42, 34, and 24 percent for the first, second, and third stages, respectively. The corresponding stage efficiencies were 0.904, 0.851, and 0.806. The over-all turbine efficiency was 0.874.

High loss regions were found near the hub and tip regions for all three rotors, particularly for the third stage. Stator and rotor blade design diffusion numbers were calculated based on blade geometry and a stream-filament analysis. The calculated values of design diffusion correlated the blade losses to the extent that high stator and rotor diffusions for the third stage resulted in high losses for the third stage. The first and second stages agreed reasonably well. However, no spanwise correlation of blade losses with diffusion for any of the three stages was observed.

INTRODUCTION

As a part of a general study of high-work-output low-speed multistage turbines, an experimental investigation of three-stage Type II turbines for the J71 turbojet engine is being conducted at the NACA Lewis laboratory. Two different turbines were constructed, the Type IIF and the Type IIA. Although both turbines were geometrically similar, having the same annular flow variation through the turbine and the same number of blades in corresponding blade rows, the IIA turbine had smaller blade throat areas for all blade rows downstream of the first stator. In addition, the blading of the IIA turbine was of the curved-back type; that is, the blade profiles had curvature on the suction surfaces downstream of the blade throats. The IIF turbine employed straight-backed blades. The over-all

CLASSIFICATION CANCELLED
Authority NACA PUBLICATIONS
ANNOUNCEMENTS NO.
Date By

component performance results of these two turbines are presented in references 1 and 2; and a comparison of results indicated the IIA turbine, in general, performed slightly better than the IIF turbine at comparable operation conditions. However, the difference in turbine efficiencies at design speed and work output was small, both configurations producing efficiencies of about 0.88.

A detailed study of the internal flow conditions of the J71 Type IIF turbine was then conducted at the equivalent design speed and near the equivalent design work output (ref. 3). This study was based on radial survey instrumentation located behind each blade row. Although the results as presented were not intended to be quantitative because of inherent circumferential flow variations, they can be interpreted as indicating trends of comparative performance of a turbine blade row or stage. The investigation revealed that the stage-work distribution closely approximated that of design. The first-, second-, and third-stage efficiencies were 0.894, 0.858, and 0.792, respectively. The fact that the third-stage rotor was unshrouded and had a relatively large tip clearance was believed to be a contributing factor toward the low efficiency of the third stage. As a consequence, the third-stage rotor was shrouded, and this modified IIF turbine was experimentally investigated. The results are presented in reference 4. It was found that shrouding the third rotor had a negligible effect on over-all turbine efficiency.

Because the over-all efficiencies of the IIF and IIA turbines were comparable, it was considered of interest to perform an experimental survey study of the IIA turbine, similar to that for the IIF turbine, in order to ascertain the individual stage performance characteristics. It is conceivable that the individual stage efficiencies of the IIA turbine could vary considerably from those that existed in the IIF turbine (ref. 3), and still the two turbines could yield the observed comparative over-all efficiencies. It is also considered of importance to determine whether the unshrouded third-stage rotor of the IIA turbine would perform in the same manner as that for the IIF unshrouded third rotor. Accordingly, the J71 Type IIA turbine was set up and instrumented similarly to the IIF turbine (ref. 3), and the unit was again operated at the design speed and near the design work output. The results obtained are presented and compared herein with those of the IIF turbine.

APPARATUS AND INSTRUMENTATION

The J71 Type IIA and Type IIF turbines are described in detail and contrasted in reference 2. Briefly, the two turbines differ in blade profile shape and blade throat areas. The blade profiles in the IIF turbine were straight-backed, whereas the IIA turbine employs curve-backed blades. Furthermore, the IIA turbine had smaller blade throat areas in all blade rows downstream of the first stator than the IIF turbine.

The over-all experimental setup used for the subject investigation of the IIA turbine was essentially the same as described in reference 1 for testing the Type IIF turbine. A photograph of the over-all experimental installation showing the various components is presented in figure 1. The installation of the interstage static-pressure taps, as well as the instrumentation necessary to determine the over-all turbine performance, is described in reference 3. Additional instrumentation included a combination total-pressure and angle probe ahead of the first stator and behind each of the three stator blade rows. Behind each rotor, two combination total-pressure, angle, and total-temperature probes were mounted in two different circumferential locations. All combination probes were mounted in remotely controlled actuators and were used to record the radial variations of the aforementioned measurements. A photograph of a representative combination probe is shown in figure 2. A schematic diagram of the IIA turbine, showing the turbine blading, the interstage instrumentation, and the circumferential location of the combination probes is presented in figure 3.

SYMBOLS

The following symbols are used in this report:

- A annular area, sq ft
- D diffusion factor, $(W_{\max} - W_e)/W_{\max}$
- g acceleration due to gravity, 32.174 ft/sec²
- p pressure, lb/sq ft or in. Hg abs
- R gas constant, 53.4 ft-lb/(lb)(°R)
- r radius, ft
- T temperature, °R
- U wheel speed, ft/sec
- V absolute gas velocity, ft/sec
- W relative gas velocity, ft/sec
- α absolute flow angle (measured from axial direction), deg
- β relative flow angle (measured from axial direction), deg
- γ ratio of specific heats

η	adiabatic efficiency
ρ	gas density, lb/cu ft
σ	solidity, ratio of actual blade chord to blade spacing
ω	angular velocity, radians/sec
$\bar{\omega}$	loss coefficient

Subscripts:

av	mass-averaged value
c	calculated
e	exit
i	inlet
max	maximum, local
u	tangential
x	axial
0,1,2,3, 4,5,6,7	measuring stations (see fig. 3)

Superscripts:

'	stagnation or total state
"	relative stagnation or total state

PROCEDURE AND CALCULATIONS

The equivalent design conditions of the J71 Type IIA turbine, based on standard NACA sea-level turbine-inlet pressure (29.92 in. Hg abs) and temperature (518.7° R), were 32.4 Btu per pound for the work output, 40.3 pounds per second for the weight flow, and 3028 rpm for the speed. The experimental turbine was operated at this equivalent design point with an inlet pressure of 35 inches of mercury absolute and an inlet temperature of 700° R. Based on the torque measurements, the brake internal efficiency of this point was 0.879, which compares very closely to the efficiency of 0.880 as observed in reference 2 at equivalent design speed and work.

With the turbine speed, pressure ratio, and inlet conditions maintained fixed, each combination probe was individually operated radially from tip to hub. A sufficient number of points were observed to define the trends of temperature (at the rotor exits only), pressure, and flow angle for each of the ten probes. This procedure was slightly different from that used during the investigation of reference 3, because (1) more readings were observed, and (2) the temperature measurements were made in the same circumferential locations as were the pressure and angle measurements. These temperatures were then corrected for Mach number recovery. Where duplicate instrumentation existed, the measurements were numerically averaged at their corresponding radial positions.

It is recognized that circumferential flow variations prevail behind a blade row. Only radial measurements were obtained during the subject investigation because of the extreme complexity of incorporating provisions for circumferential survey instrumentation. Although all combination probes (as well as the static taps) were located midway between two adjacent stator blades, the observed readings may have been influenced by upstream blade wakes. Exactly the same limitations were expressed and considered in the survey investigation of the IIF turbine (ref. 3). The results presented herein are not, then, to be considered quantitative; however, they can be interpreted to indicate trends of comparative stage performance. Furthermore, since the same limitations were imposed on the IIF turbine, and because the instrumentation for the two turbine configurations was similar, a reasonable comparison between the two turbines can be expected.

The results are presented in terms of a work-output parameter $\Delta T'/T'$ and adiabatic efficiency η of a stage where local values of pressures and temperatures were evaluated along an assumed streamline passing through a given percentage of annular area at any given measuring station. Both of these parameters were also numerically integrated to obtain mass-averaged values for each stage as well as across the entire three stages. In addition, local values of total pressure, static pressure, and total temperature were used to calculate the absolute flow Mach numbers and velocities. From the observed flow angle, components of these velocities, V_x and V_u , were then determined. With these values and the known wheel speed U , relative flow velocities, Mach numbers, and angles were computed. To check the accuracy of the calculated flow velocities, local values of $\Delta T'/T'$ were computed from the known wheel speed and the change in the tangential velocity ΔV_u across a rotor blade row. The agreement between the measured and the computed $\Delta T'/T'$ is an indication of the validity of the flow measurements and assumptions used to calculate flow velocities and angles.

As stated previously, static pressures were observed at the hub and tip ahead of and behind each blade row. A linear radial variation was

assumed at a particular measuring station in order to calculate absolute Mach numbers of the flow. At measuring station 3, however, the tip value of static pressure was considerably lower than the hub value, which is contradictory to the consideration of simple radial equilibrium. Because the measured static pressure across the hub of the first rotor closely approximated the design value as computed from the velocity diagrams (fig. 4), whereas the observed tip values of static pressure disagreed considerably from design, the observed static pressures at the hub were considered correct. This hub value was then arbitrarily assumed constant along the blade height. Similar static-pressure variations were also noted at measuring stations 4 and 5, but only to a smaller extent, so that the observed values were considered representative and the linear variation was used.

A stage loss coefficient $\bar{w} \cos \beta_e / \sigma$ developed in reference 3 and a design diffusion factor D for the rotor blades and stator blades are also included herein. For the convenience of the reader, the equations used to calculate all parameters are listed in the appendix.

RESULTS AND DISCUSSION

Design Considerations

The J71 Type IIA turbine design vector diagrams are presented in figure 4. The turbine design has Mach numbers on the order of 0.47 entering all three rotor rows of blades at the hub. Also, the maximum design rotor turning angle was $109^\circ 36'$, occurring across the hub section of the first rotor. Low turbine-exit tangential velocities and discharge Mach numbers prevail at the exit of the third rotor. In addition, the turbine design incorporates accelerating flow across each blade row. All these criteria indicate a conservative design. The IIA turbine performed reasonably well, as found in the over-all turbine investigation (ref. 2), since the efficiency at the equivalent design speed and work was 0.880. Design equivalent weight flow was also attained at this operating point. Comparable efficiency characteristics were obtained in the over-all performance investigation of the J71 Type IIF turbine (ref. 1), although the level of efficiencies was slightly less than that for the IIA turbine (ref. 2).

The IIF turbine was designed with straight-backed blades, whereas the IIA turbine employed curve-backed blades. From structural considerations, the curve-backed blades permitted thicker blade sections just upstream of the blade trailing edges, and, hence, should have longer life and less distortion under actual engine operating conditions. Aerodynamically, and within the limits of curvatures used on the IIA turbine blades, reference 5 indicates that the selection of blade shape has no appreciable effect on

blade losses at the Mach number level for which both turbines were designed. In fact, design Mach numbers entering all blade rows of the IIA turbine were slightly less than those for the corresponding blade rows of the IIF turbine. A maximum difference in Mach number of 0.068 occurred at the turbine discharge, the IIF turbine again having the higher Mach numbers. In addition to Mach number considerations, the IIA turbine design requires more turning in the rotors than that for the IIF turbine, particularly in the third stage, where this difference amounted to 10° at the hub.

Figure 5 shows typical blade sections and channels near the hub, mean, and tip for all three stages of J71 Type IIA turbine. The aforementioned curve-backed blade contours can be noted by the curvature of the suction surface downstream of the blade throats.

Stage Performance

The individual stage and the over-all performance results of the J71 Type IIA turbine are presented in figure 6, which shows the variation of work parameter $\Delta T'/T'$ and efficiency η with percent of annular area. The mass-averaged values of the work-output parameter are 0.1071, 0.0950, and 0.0792, for the first, second, and third stages, respectively. These values represent 42, 33, and 25 percent, respectively, of the over-all turbine work output, and compare very closely with the design values of 42, 34, and 24 percent. The over-all mass-averaged work parameter was 0.2555.

As to the radial variation of the stage work, figure 6 shows work deficiencies near the hub and tip for all three stages. This is, of course, reflected in the over-all turbine $\Delta T'/T'$ curve. The third stage shows a severe decrease in work near the tip. The same condition was noted in the corresponding investigation of the J71 Type IIF turbine tests reported in reference 3. The fact that the third rotor was unshrouded and had a relatively large tip clearance was believed to be a contributing factor toward this low work output near the tip region of the blade. A subsequent investigation was conducted on the IIF turbine in which this third-stage rotor was shrouded (ref. 4); however, no improvement in over-all turbine performance was noted with this modification. It should be stated, however, that the third stages of both the IIF and the IIA turbines were designed to produce less than 25 percent of the total turbine work. Hence, from an over-all turbine performance evaluation, a significant improvement in the performance of the third stage of either turbine is required to improve the over-all performance of the turbine.

Also shown in figure 6 are the curves of $\Delta T'/T'$ for the Type IIF turbine. The similarity of trends for the first stage, the third stage, and the over-all work-parameter curves for the two turbine configurations can be noted readily. It appears that the second stage of the IIF turbine (ref. 3) had a more uniform work-parameter distribution over the blade height than did the IIA turbine. However, no direct comparison of the

absolute values of $\Delta T'/T'$ for the two turbines is made, since the IIA turbine was operated at an equivalent work of 32.35 Btu per pound, whereas the IIF turbine was operated at 31.1 Btu per pound (ref. 3).

The calculated work parameters $(\Delta T'/T')_c$ are also shown in figure 6. In general, the trends of the calculated and experimental curves of $\Delta T'/T'$ agree reasonably well for all three stages. The absolute values, however, indicate the calculated values of $\Delta T'/T'$ are generally higher than the measured values. The absolute level for the first stage shows good agreement between the calculated and measured values of work parameter. The agreement of the second stage is fair. The third stage indicates good agreement in the lower half of the blade span, but rather poor agreement in the upper half of the blade, where the order of the deviation amounted to over 20 percent.

The performance of the Type IIA turbine can also be compared with that of the IIF turbine by referring to the efficiency curves, which are also presented in figure 6. Low-efficiency regions can be noted near the hub and tip for all three stages, resulting in the same general trend for the over-all turbine efficiency. The mass-averaged values of efficiency for the first, second, and third stages are 0.904, 0.851, and 0.806, respectively. The corresponding values for the IIF turbine (ref. 3) were 0.894, 0.858, and 0.792. The integrated over-all efficiency for the IIA turbine was 0.874, whereas that of the IIF turbine was 0.868. The trend in stage efficiencies for the two turbines were similar; that is, the third-stage efficiencies were lower than those of the second stage, and the second-stage efficiencies were lower than those of the first stage. The spanwise variation as well as the integrated over-all and stage efficiencies for both turbines correlated closely, lending credence to the over-all survey results. Furthermore, these performance similarities indicate that, within the Mach number levels encountered in these turbines, both straight-backed and curve-backed blading performed equally well.

Stage Flow Mach Numbers and Angles

The spanwise variation of the absolute and relative flow Mach numbers and angles entering and leaving each rotor row of blades is presented in figure 7. Design values are also shown, the values being selected from the design vector diagrams in figure 4. Flow angles measured in the direction of rotor rotation are considered positive on the angle plots. Figure 7(a), which shows the Mach numbers and flow angles entering and leaving the first-rotor row of blades, indicates that the measured values of the entrance absolute and relative Mach numbers are considerably higher than design, and the rotor-exit relative and absolute Mach numbers are lower than design. Hence, design reaction in terms of Mach number across

the rotor was not attained. The flow angle out of the first stator was reasonably close to that of design, except in the blade end regions, where underturning existed. The rotor-entrance relative flow angles were less than design near the hub, and greater than the design value over most of the blade span. At the first-rotor exit, the relative flow angle was close to design except near the hub, where overturning existed. In the absolute frame, the exit flow was some 6° to 10° less than design except near the hub. These variations in angle from design result in off-design angles of incidence on the following blade rows, and can result in increased blade losses. Incidence angle is herein considered to be the difference between the measured angles and the corresponding angles given by the vector diagram (fig. 4).

The entrance and exit Mach numbers and angles for the second rotor are shown in figure 7(b). As for the first rotor, the entrance absolute and relative Mach numbers are greater than design over the entire blade span. The second-rotor-exit Mach numbers were higher than design except in the blade end regions. The variation of these Mach numbers from design can be ascribed partly to the fact that the calculated velocities are higher than those which actually exist in the turbine, since the calculated work $(\Delta T'/T')_c$ for the second stage was higher than the measured work $(\Delta T'/T')$, as shown in figure 6. Both the entrance and exit flow angles approximate design conditions except in the blade end regions. The exit absolute angle is some 4° to 10° less than design at the blade tip, and this variation indicates a negative angle of incidence on the succeeding row of blades, the third stator.

Figure 7(c) presents the flow conditions entering and leaving the third-rotor row of blades. As found for the first two rotors, the entrance Mach numbers to the third rotor are considerably higher than the design values all along the blade span. The exit relative Mach number is higher than design in the midspan region, but lower at the blade extremities. The exit absolute Mach number, however, agreed with design values except at the end regions again, where, in general, the Mach numbers were less than design. Fair agreement with design values was observed with the absolute and relative flow angles entering the third rotor and with the third-rotor-exit relative flow angles. The exit absolute flow angle was some 5° to 10° more negative than the design value over the main portion of the blade. The blade end regions again deviate from the main flow angle.

Stage Loss Function and Design Blade Diffusion

Figure 8 presents the variation of a stage loss function $[(\bar{\omega} \cos \beta)/\sigma]_e$ and design values of diffusion D on the suction surface of the rotor and stator blades as functions of the annular area. The loss function was calculated from the rotor blade geometry and the flow measurements at the exit of each stage. It is immediately apparent

that the loss function is greater near the hub and tip than in the midspan of the rotor blades for all three stages. Also, the level of the loss function for the third stage is higher than for the first or second stages, which have approximately similar loss levels. The third stage also has a much more limited range of low losses in the midspan region.

The curves showing the variation of design diffusion with percent of annular area for all three rotors and stators are also shown in figure 8. These diffusion values do not represent experimental values that actually are encountered in the turbine. In fact, design diffusion cannot be expected, since the design vector diagrams were not established at the design equivalent operating point at which these survey data were obtained. However, if the design diffusion values are considered as an indication of the actual blade diffusion, then high values of diffusion should indicate high blade losses. No such spanwise correlation is indicated in figure 8 for any of the three stages. In fact, the converse seems to prevail. It can be noted, however, that the levels of the rotor and stator diffusion curves for the third stage are higher than those of the first and second stages, as was observed for the loss-function curves (fig. 8). Arbitrarily, then, the individual stage loss-function curves were mass-averaged, and the design diffusion curves were area-averaged. These average values are shown in figure 9. It is readily apparent that the averages of the third-stage design diffusion and loss function are considerably higher than those observed for the first or second stage. These data indicate that, based on average stage diffusion and loss function, high design diffusion results in high stage losses and, hence, lower stage efficiencies.

SUMMARY OF RESULTS

From an investigation of the internal flow conditions of the J71 Type IIA three-stage turbine, operated at the equivalent design speed and work output, the following results were obtained:

1. The mass-averaged values of efficiency for the first, second, and third stages of the turbine were 0.904, 0.851, and 0.806, respectively. The corresponding turbine over-all efficiency was 0.874.
2. The first stage of the turbine produced 42 percent of the total turbine work, the second stage 33 percent, and the third stage 25 percent. These values closely correlate design values of 42, 34, and 24 percent for the first, second, and third stages, respectively.
3. High loss regions prevailed near the hub and tip for all three rotors, particularly for the third stage.

4. Design diffusion and blade losses correlated to the extent that high stator and rotor diffusion for the third stage resulted in high losses for the third stage. No spanwise correlation of blade losses with diffusion for all three stages was observed, however.

Lewis Flight Propulsion Laboratory
National Advisory Committee for Aeronautics
Cleveland, Ohio, August 8, 1955

APPENDIX - EQUATIONS USED TO CALCULATE TURBINE

PERFORMANCE PARAMETERS

The equations used to calculate the various flow parameters are as follows for the first stage of the turbine:

$$\frac{\Delta T'}{T'} = 1 - \frac{T'_3}{T'_0} \quad (1)$$

$$\eta = \frac{1 - \frac{T'_3}{T'_0}}{1 - \left(\frac{p'_3}{p'_0}\right)^{\frac{\gamma-1}{\gamma}}} \quad (2)$$

$$\left(\frac{\Delta T'}{T'}\right)_{av} = \frac{\int_0^A \left(1 - \frac{T'_3}{T'_0}\right) \rho_3 V_{x,3} dA_3}{\int_0^A \rho_3 V_{x,3} dA_3} \quad (3)$$

$$\eta_{av} = \frac{\int_0^A \left[\frac{1 - \frac{T'_3}{T'_0}}{1 - \left(\frac{p'_3}{p'_0}\right)^{\frac{\gamma-1}{\gamma}}} \right] \rho_3 V_{x,3} dA_3}{\int_0^A \rho_3 V_{x,3} dA_3} \quad (4)$$

$$\left(\frac{\Delta T'}{T'}\right)_c = \frac{\omega(r_2 V_{u,2} - r_3 V_{u,3})}{\frac{\gamma}{\gamma-1} g R T'_0} \quad (5)$$

$$\bar{\omega} = \frac{p_2'' - p_3''}{p_2'' - p_3} \quad (6)$$

Equation (6) is defined and developed in the appendix of reference 3. Equations (1) to (4) are concerned with the entire stage, that is, across the first-stage stator and rotor. Equations (5) and (6) concern only the rotor, except for the stage-inlet temperature in the denominator of equation (5), which was assumed constant across the stator. The same equations were used to calculate the performance parameter of the second and third stages, with appropriate changes in the measuring-station subscript nomenclature (see fig. 3). In all cases, local values of observed pressures, angles, and temperatures were used except for the turbine-inlet temperature T'_0 , which was assumed constant across the first-stator blade span. Equations (1) to (4) were also calculated across the entire turbine, from station 0 to station 7.

In addition, a diffusion factor D for each turbine blade row was computed from the equation

$$D = \frac{W_{\max} - W_e}{W_{\max}}$$

where W_{\max} is the maximum velocity on the suction surface of the blade, and W_e is the average exit velocity within the plane of the trailing edge. The values of D were computed from the design vector diagrams and the blade geometry in conjunction with the manufacturer's stream-filament analysis.

REFERENCES

1. Schum, Harold J., and Davison, Elmer H.: Component Performance Investigation of J71 Type II Turbines. I - Over-All Performance of J71 Type IIF Turbine with 97-Percent-Design Stator Areas. NACA RM E54J15, 1954.
2. Schum, Harold J., Davison, Elmer H., and Petrash, Donald A.: Component Performance Investigation of J71 Type II Turbines. III - Over-All Performance of J71 Type IIA Turbine. NACA RM E55A20, 1955.
3. Rebeske, John J., Jr., and Petrash, Donald A.: Component Performance Investigation of J71 Type II Turbines. II - Internal Flow Conditions of J71 Type IIF Turbine with 97-Percent-Design Stator Areas. NACA RM E54L16, 1955.
4. Petrash, Donald A., Schum, Harold J., and Davison, Elmer H.: Component Performance Investigation of J71 Type II Turbines. IV - Effect of Third-Stage Shrouding on Over-All Performance of J71 Type IIF Turbine. NACA RM E55C29, 1955.

5. Ainley, D. G., and Mathieson, G. C. R.: An Examination of the Flow and Pressure Losses in Blade Rows of Axial Flow Turbines. Rep. No. R.86, British N.G.T.E., Mar. 1951.

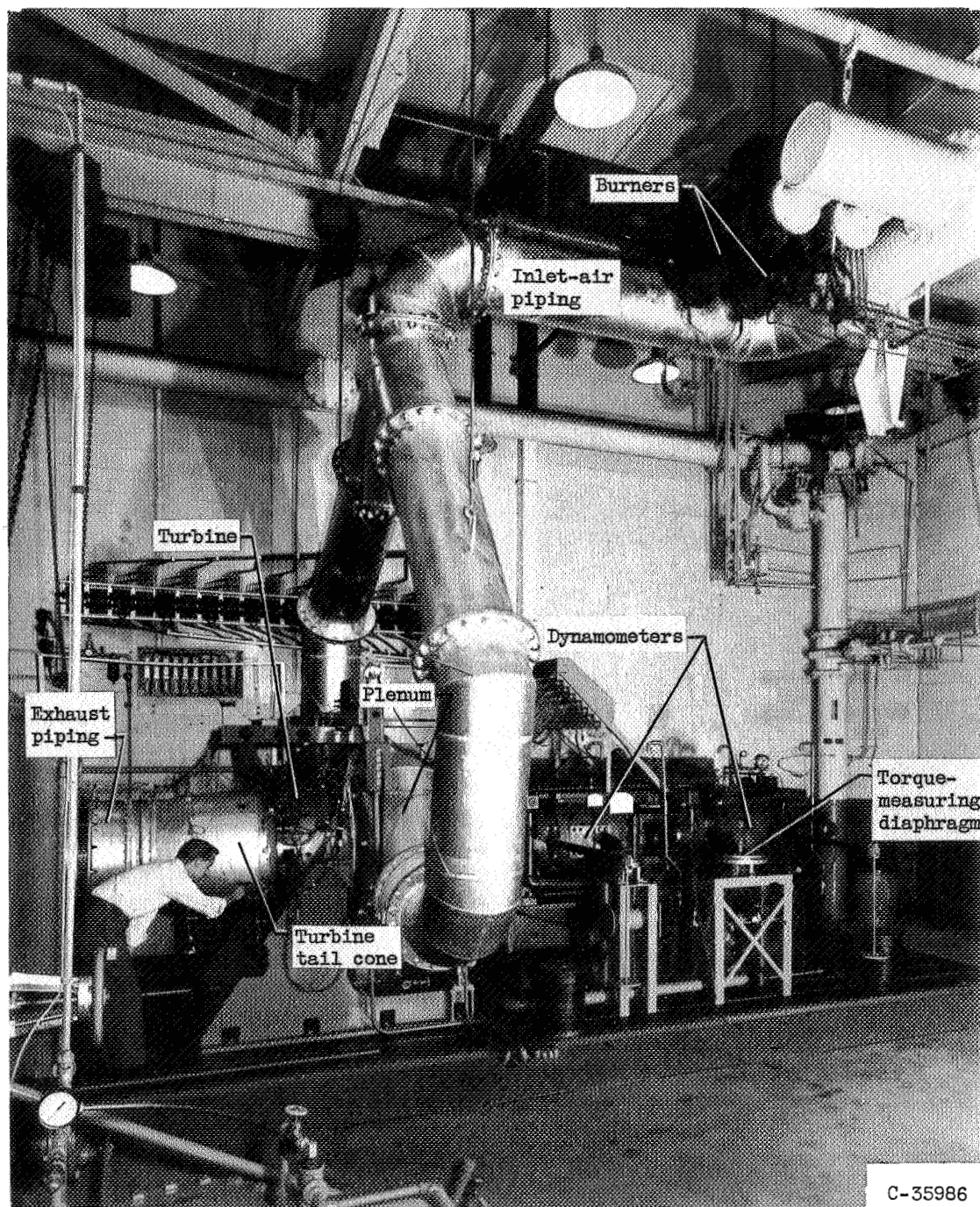


Figure 1. - Installation of J71 Type IIA three-stage turbine in full-scale turbine component test facility.

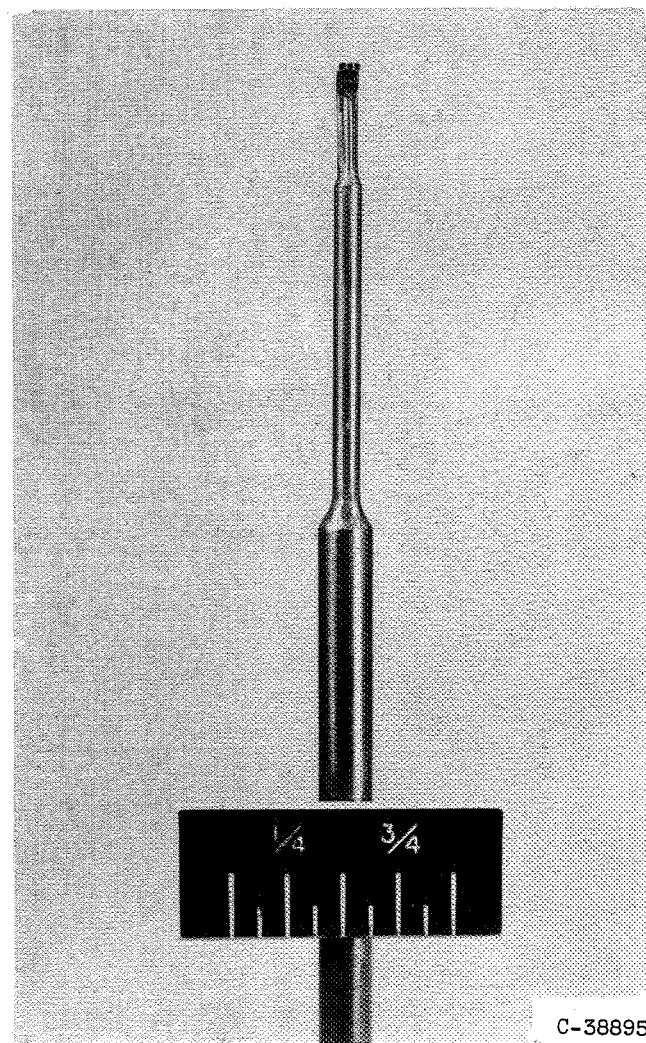
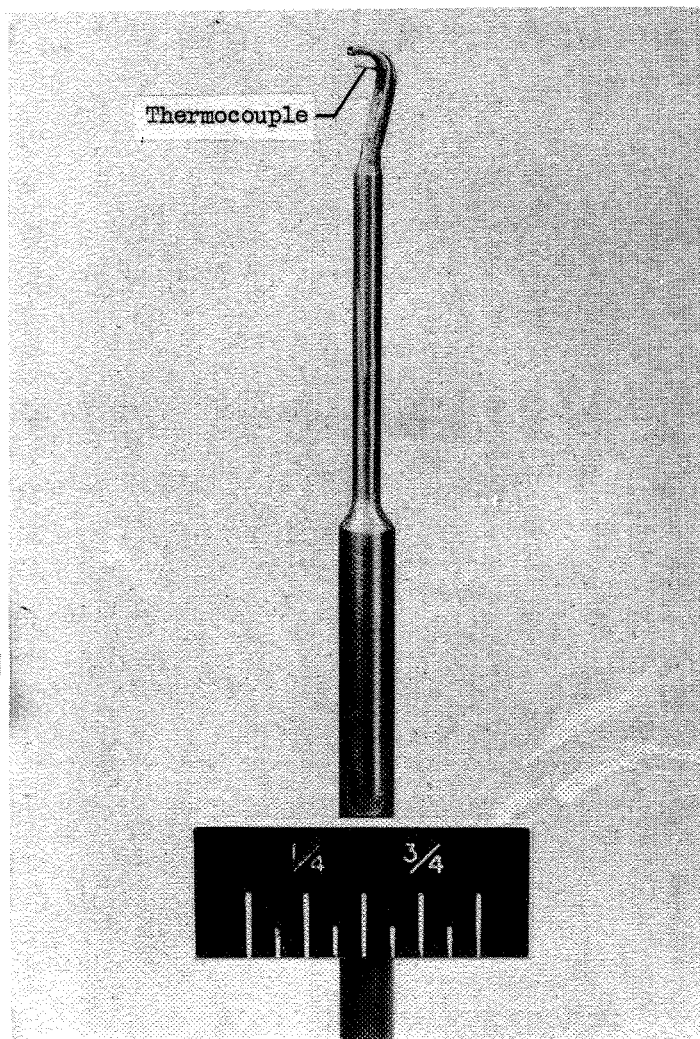


Figure 2. - Representative combination total-pressure, angle, and temperature probe.

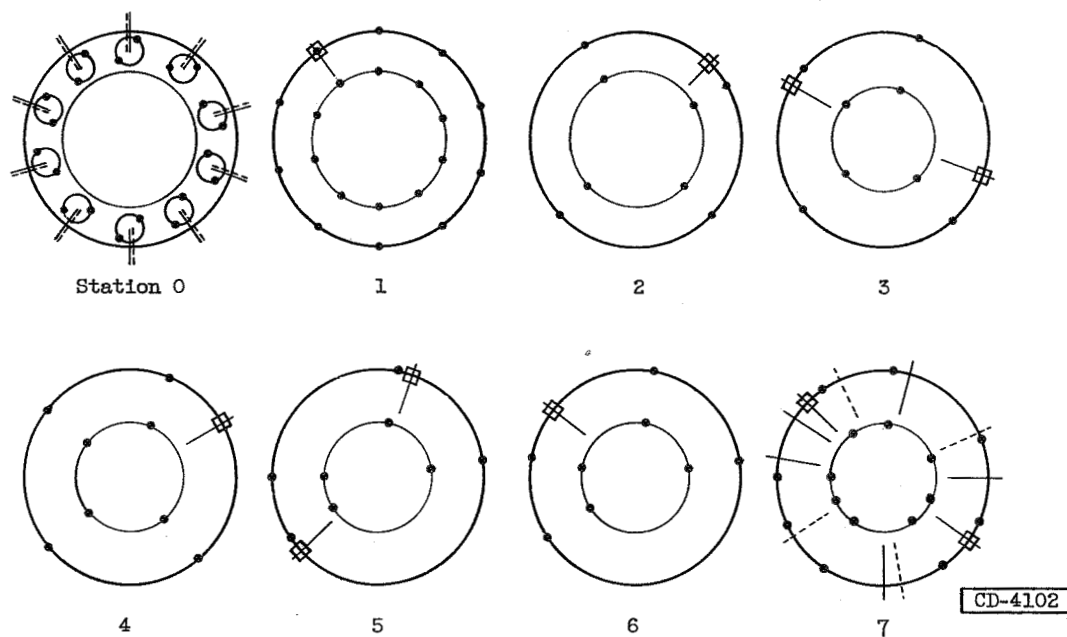
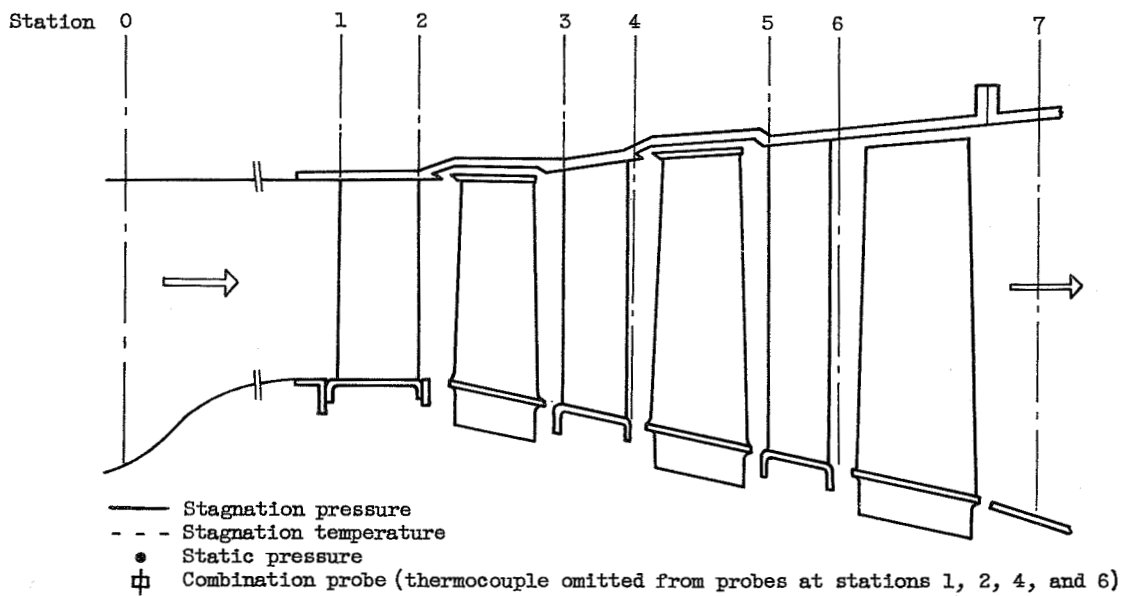
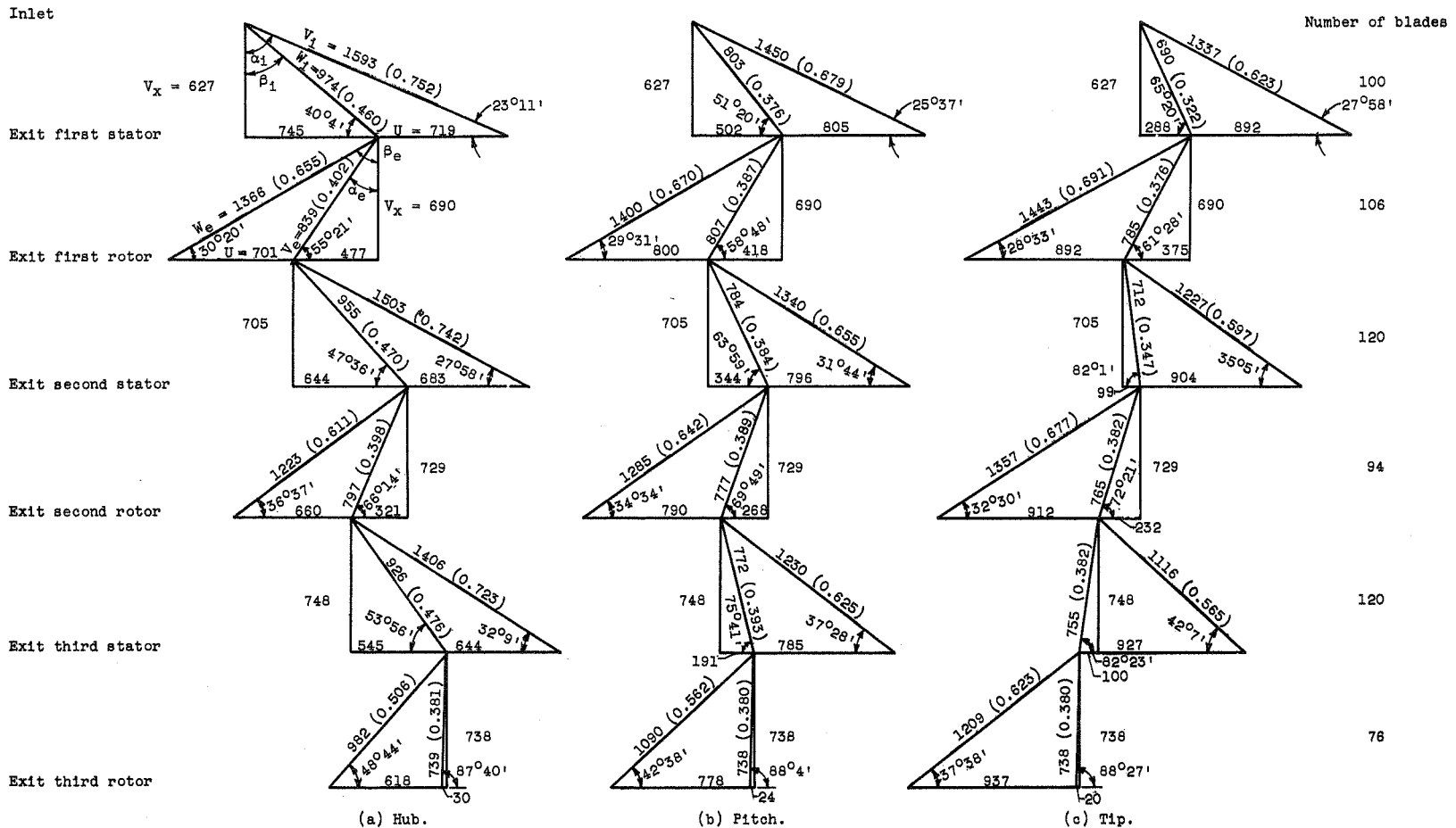
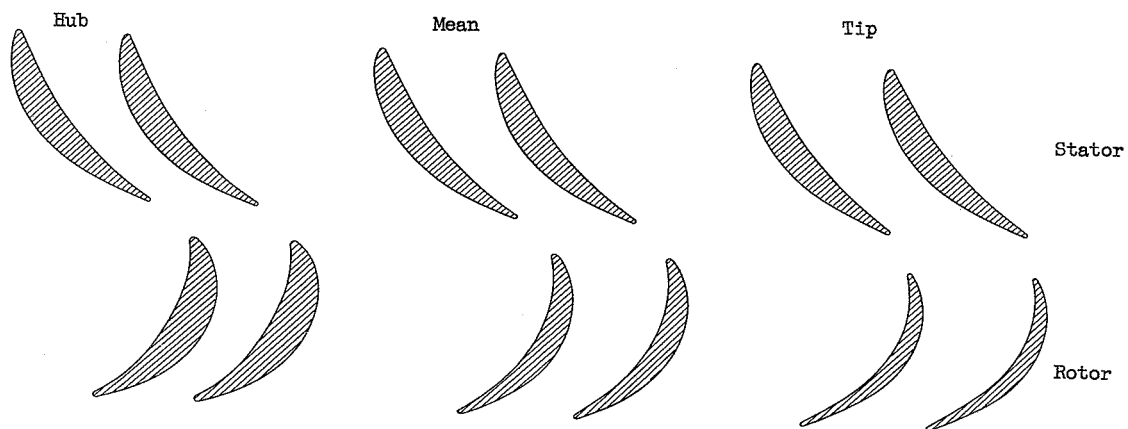
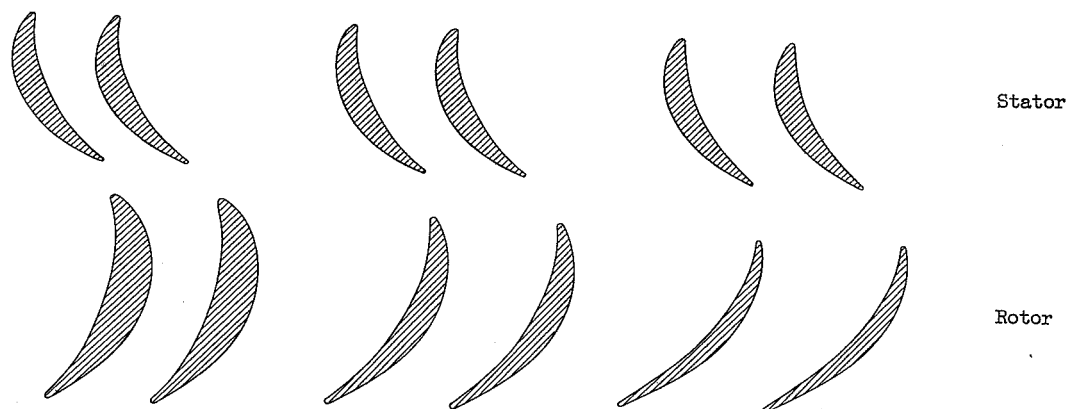


Figure 3. - Schematic diagram of J71 Type IIA turbine showing instrumentation.

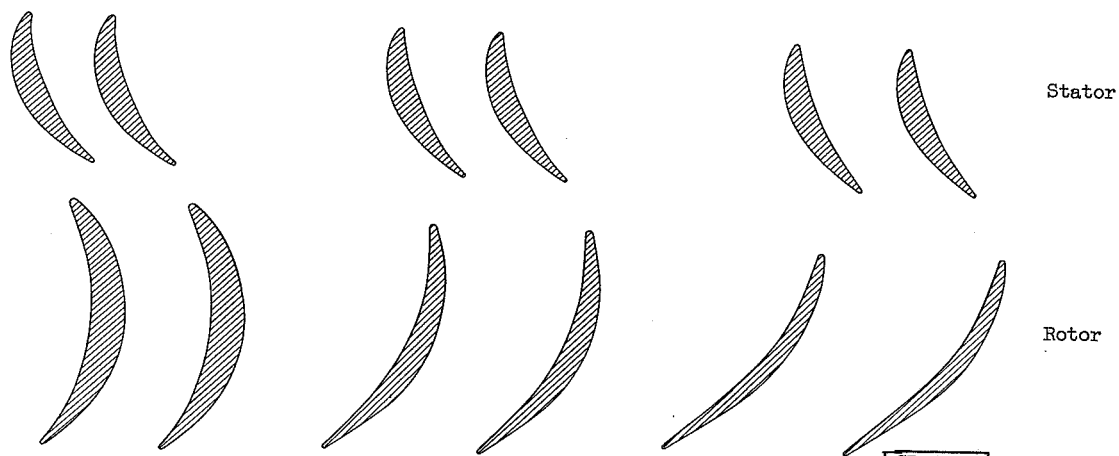




(a) First stage.



(b) Second stage.



(c) Third stage.

CD-4435

Figure 5. - Design blade and channel shapes for J71 Type IIA turbine.

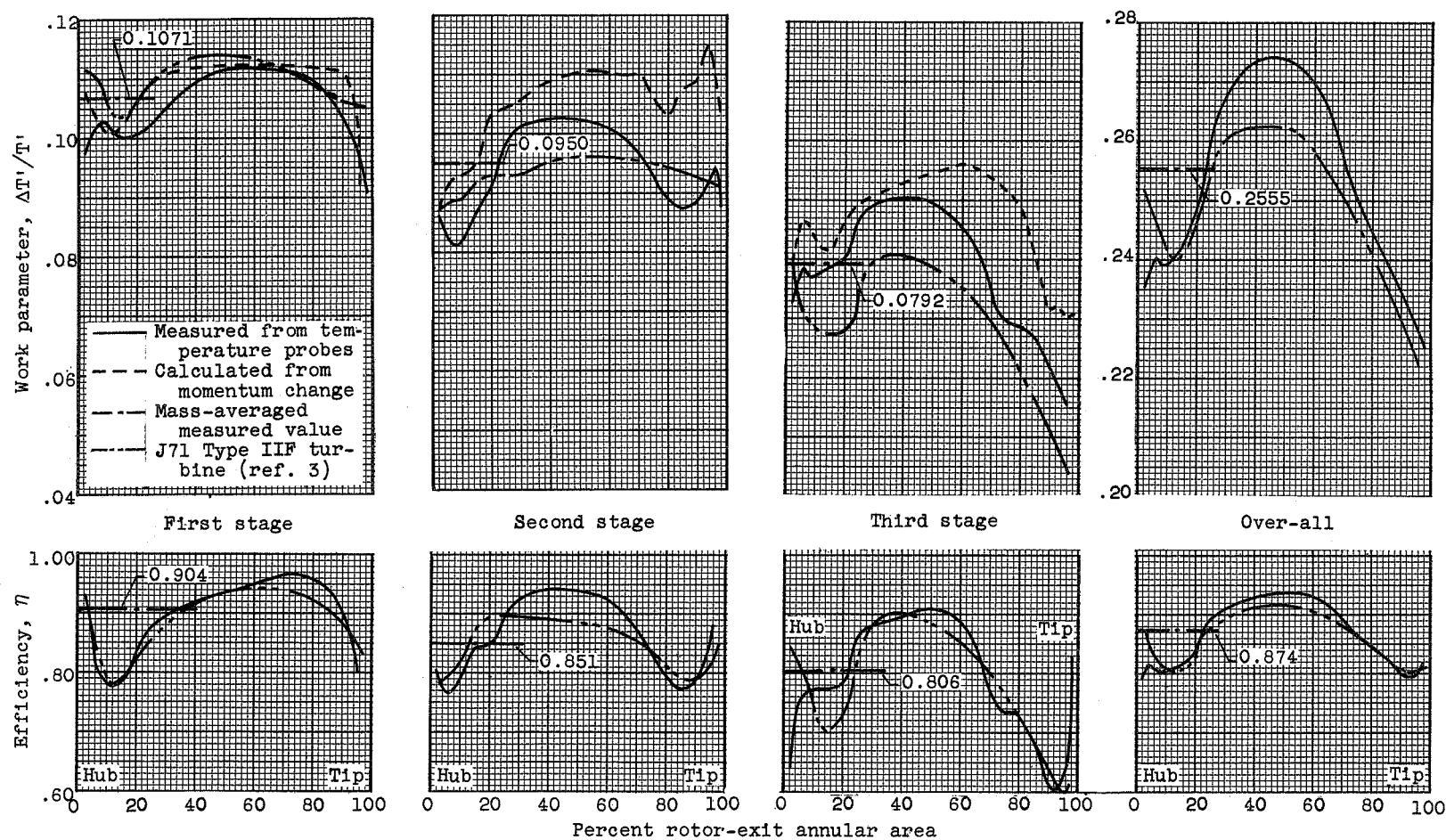
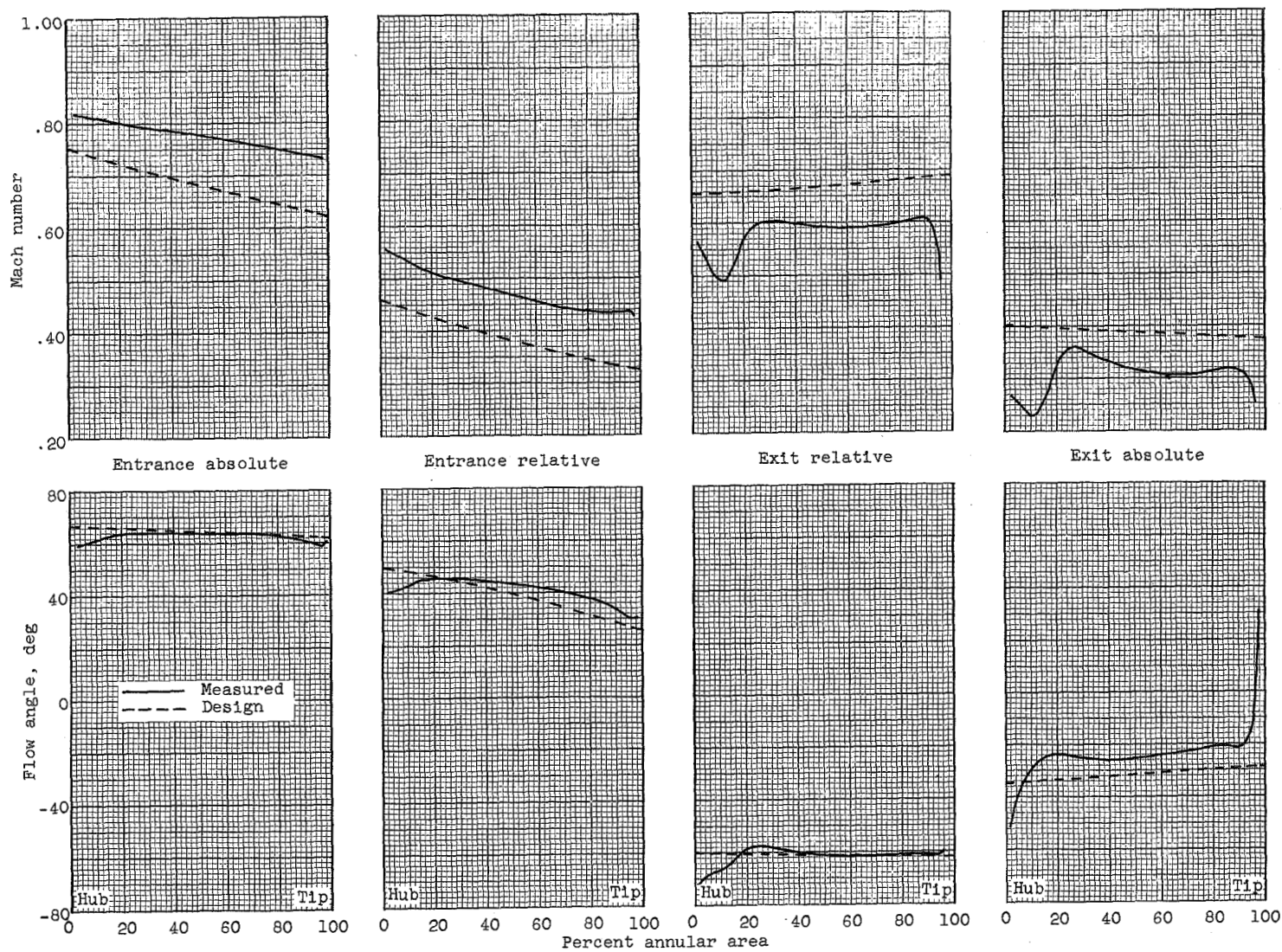
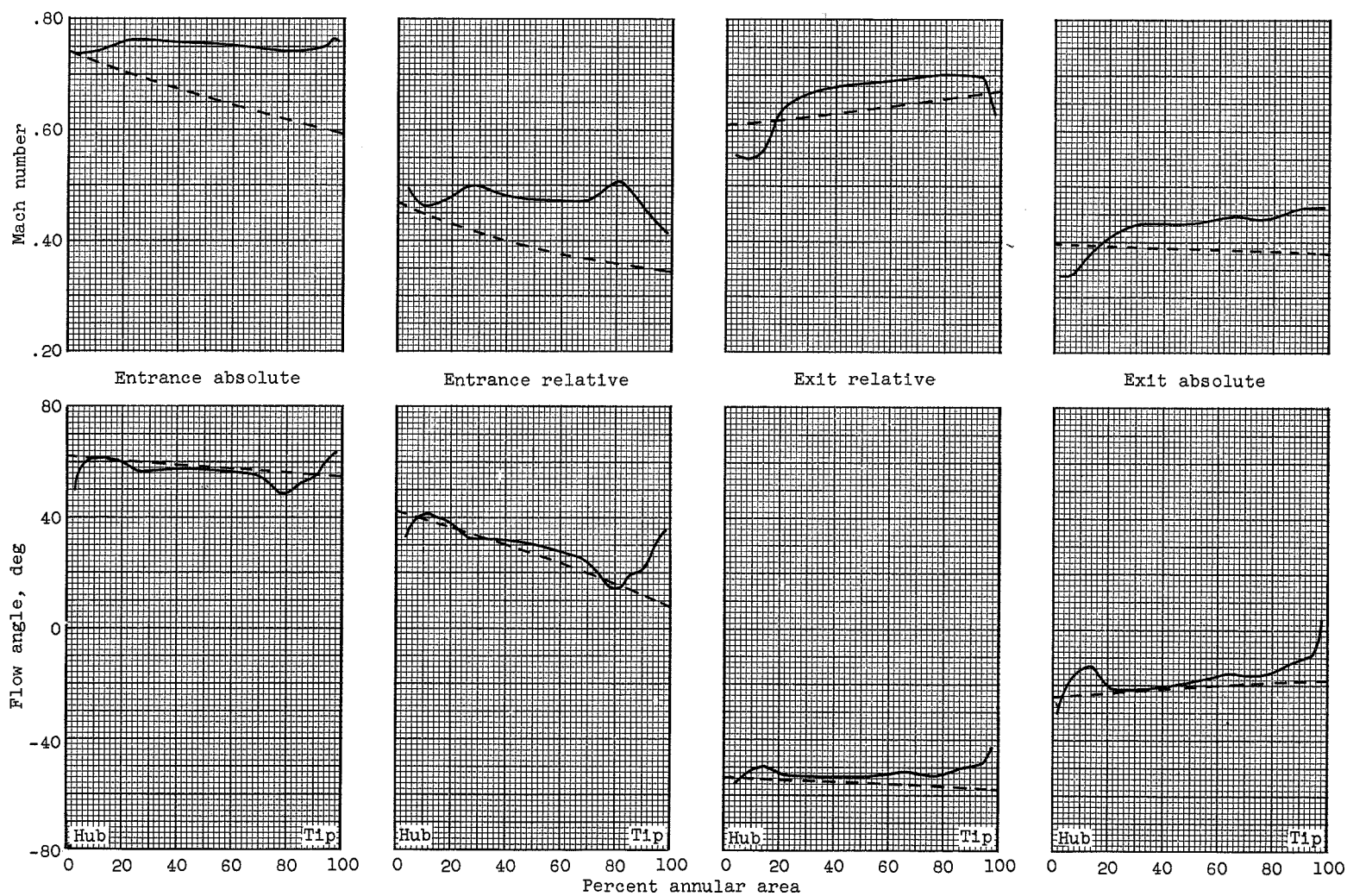


Figure 6. - Variation of stage and over-all work and efficiency of J71 Type IIA turbine with annular area at rotor exits.



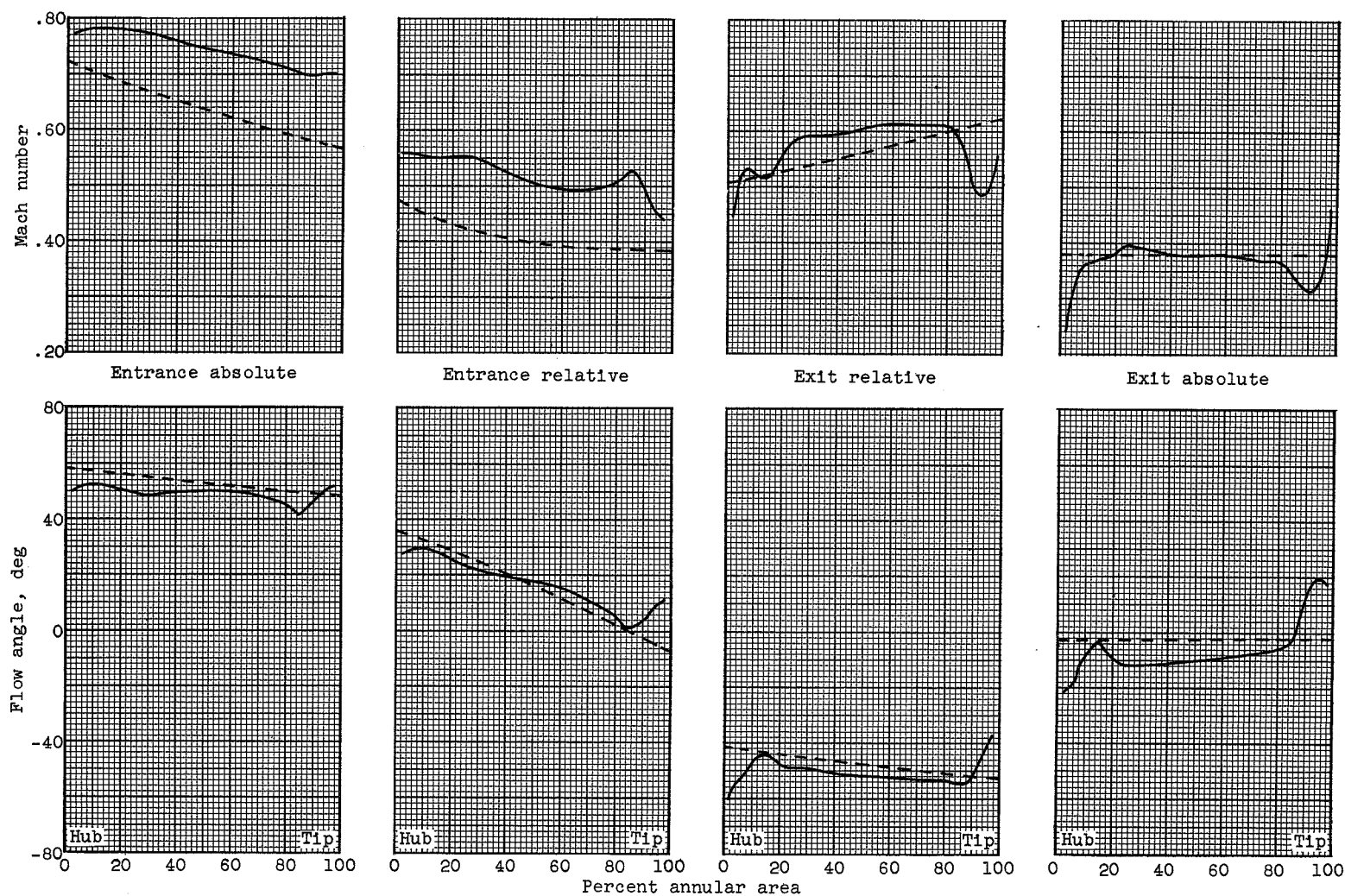
(a) First-stage rotor.

Figure 7. - Variation of absolute and relative Mach numbers and angles at rotor entrance and exit with annular area.



(b) Second-stage rotor.

Figure 7. - Continued. Variation of absolute and relative Mach numbers and angles at rotor entrance and exit with annular area.



(c) Third-stage rotor.

Figure 7. - Concluded. Variation of absolute and relative Mach numbers and angles at rotor entrance and exit with annular area.

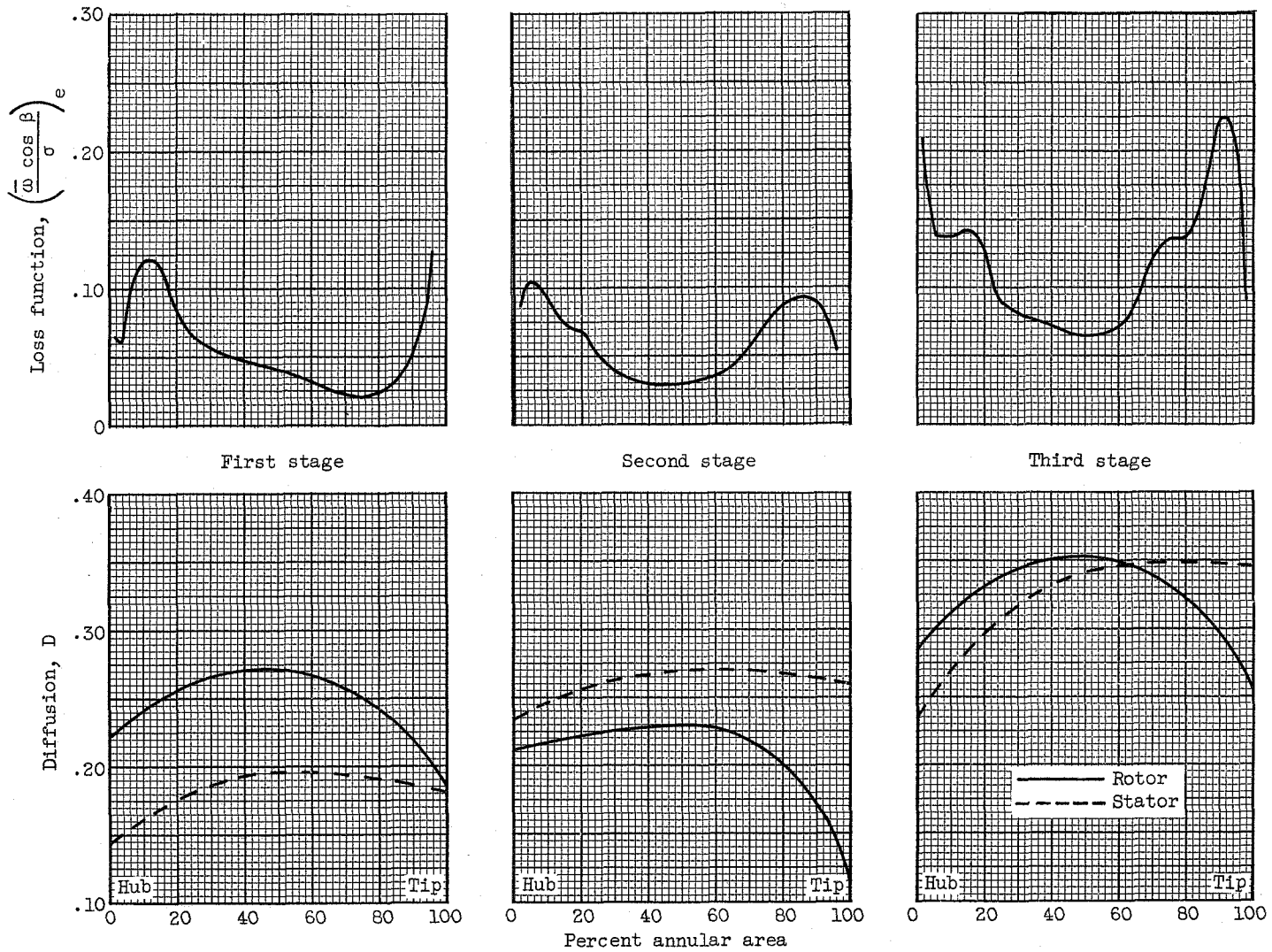


Figure 8. - Variation of loss function and design rotor and stator blade suction-surface diffusion with annular flow area for J71 Type IIA turbine.

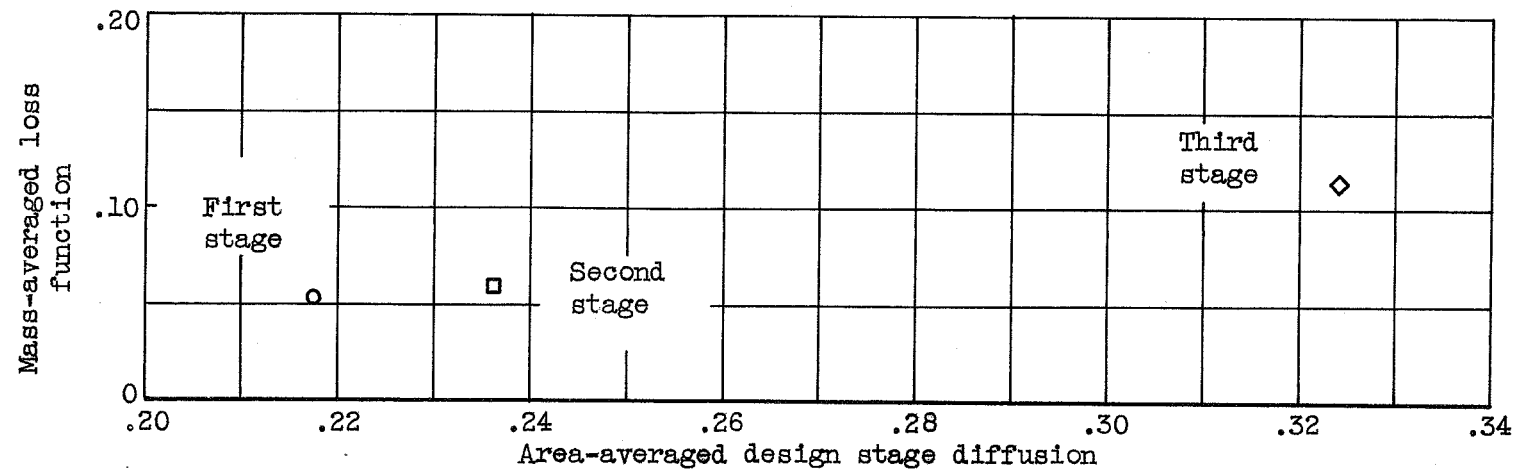
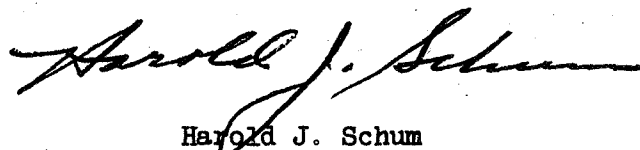


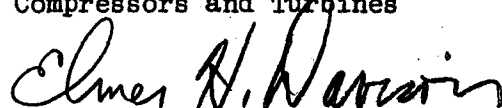
Figure 9. - Variation of average stage loss function and design diffusion.

COMPONENT PERFORMANCE INVESTIGATION OF J71 TYPE II TURBINES

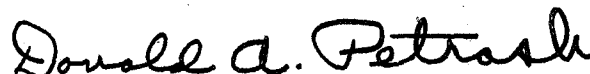
V - INTERNAL FLOW CONDITIONS OF J71 TYPE IIA TURBINE



Harold J. Schum
Aeronautical Research Scientist
Compressors and Turbines



Elmer H. Davison
Aeronautical Research Scientist
Compressors and Turbines



Donald A. Petrash
Aeronautical Research Scientist
Compressors and Turbines

Approved:

Ambrose Ginsburg
Aeronautical Research Scientist
Compressors and Turbines



Robert O. Bullock
Aeronautical Research Scientist
Compressors and Turbines

Oscar W. Schey
Chief, Compressor and Turbine
Research Division

jma - 8/8/55

Engines, Turbojet	3.1.3
Turbine Flow Theory and Experiment	3.7.1
Turbines - Axial Flow	3.7.1.1
Schum, Harold J., Davison, Elmer H., and Petrash, Donald A.	

COMPONENT PERFORMANCE INVESTIGATION OF J71 TYPE II TURBINES
V - INTERNAL FLOW CONDITIONS OF J71 TYPE IIA TURBINE

Abstract

An experimental investigation of the J71 Type IIA turbine was conducted at the equivalent design speed and work output. The design stage-work distribution was closely approached, although the design vector diagram was not attained. Efficiencies of 0.904, 0.851, and 0.806 were obtained for the first, second, and third stages, respectively. Losses occurred near the hub and tip for all three rotors. The third-stage losses, however, were significantly greater than those of either the first or second stage.